VI. References

[1] H. Hasegawa and D. G. Pettifor, *Phys. Rev. Lett.* 50, 130 (1983).

[2] G. J. Johanson, M. B. McGirr, and D. A. Wheeler, *Phys. Rev.* B1, 3208 (1970).

[3] M. F. Onellion, C. L. Fu, M. A. Thompson, J. L. Erskine, and A. J. Freeman, *Phys. Rev.*B33, 7322 (1986).

[4] C. Rau, C. Schneider, G. Xing, and K. Jamison, *Phys. Rev. Lett.*57, 3221 (1986).

[5] D. Pescia, G. L. Bona, A. Vaterlaus, R. F. Willis, and F. Meier, *Phys. Rev. Lett.*58, 2126, (1987).

[6] G. W. Fernando, Y. C. Lee, P. A. Montano, B. R. Cooper, E. R. Moog, H. M. Naik, and S. D. Bader, *J. Vac. Sci. Technol.* A5, 882 (1987).

[7] P. A. Montana, G. W. Fernando, B. R. Cooper, E. R. Moog, H. M. Naik, S. D. Bader, Y. C. Lee, Y. N. Darici, H. Min, and J. Marcano, *Phys. Rev. Lett.*59, 1041 (1987).

[8] A. Amiri Hazaveh, G. Jennings, D. Pescia, R. F. Willis, K. Prince, M. Surman and, A. Bradshaw, *Solid State Comm.*57, 329 (1986).

[9] W. Becker, H. D. Pfannes, and W. Keune, *J. Magn. Mat.* 35, 53 (1983).

[10] R. Halbauer and U. Gonser, *J. Magn. Mat.* 35, 55 (1983).

[11] J. Kübler, *Phys. Lett.* 81A, 81 (1981).

[12] O. K. Andersen, J. Madsen, U. K. Poulsen, O. Jepsen, and J. Kollar, *Physica* 86-88B, 249 (1977).

[13] D. Bagayoko and J. Callaway, *Phys. Rev.* B28, 5419 (1983).

[14] V. L. Morruzi, *Phys. Rev. Lett.* 57, 2211 (1986).

[15] F. J. Pinski, J. Staunton, B. L. Gyorffy, D. D. Johnson, and G. M. Stocks, *Phys. Rev. Lett.* 56, 2096 (1986).

[16] C. S. Wang, B. M. Klein, and H. Krakauer,*Phys. Rev. Lett.* 54, 1852 (1985).

[17] G. W. Fernando, B. R. Cooper, M. V. Ramana, H. Krakauer, and C. Q. Ma *Phys. Rev. Lett.*56, 2299, (1986) ; C. Q. Ma, M. V. Ramana, B. R. Cooper, and H. Krakauer, *Phys. Rev.*B34, 3854, (1986).

[18] S. H. Vosko, L. Wilk, and N. Nusair, *Can. J. Phys.* **58**, 1200 (1980).

[19] C. L. Fu and A. J. Freeman, *Phys. Rev.* **B35**, 925 (1987).

[20] A. J. Freeman and R. E. Watson, in *Magnetism*, edited by G. T. Rado and H. Shul (Academic, New York 1965), Vol II A.

[21] O. Gunnarsson and R. O. Jones, *Phys. Rev.* **B31**, 7588 (1985).

[22] F. J. Himpsel, J. A. Knapp, and D. E. Eastman, *Phys. Rev.* **B19**, 2919 (1979).

[23] D. E. Eastman, F. J. Himpsel, and J. A. Knapp, *Phys. Rev. Lett.* **44**, 95 (1980).

[24] E. Kisker, K. Schröder, W. Gudat, and M. Campagna, *Phys. Rev.* **B31**, 329 (1985).

Figure Captions

Fig. 1. Layer projected paramagnetic density of states for fcc iron. These have been smoothed by a Gaussian of full width at half maximum (FWHM) of 0.3 eV. The lattice constant used here is that of Cu, ($6.83a_0$). The high density of states at the Fermi level makes it an ideal candidate to satisfy the Stoner criteria.

Fig. 2. Layer projected density of states for Fe/Cu(001) and Cu(001) shown by solid and dashed lines respectively. The lattice constant and the smoothing are the same as in fig. 1. Note how the narrow Cu surface atom density of states gets broader and pushed to higher binding energies when a monolayer of iron is deposited on it.

Fig. 3. Layer projected spin-polarized density of states for fcc iron. The lattice constant and the smoothing are the same as in fig. 1. The solid lines show spin up (say) density of states while the dotted lines show the spin down density of states. Note that the surface spin up (majority) states are all occupied and also that the center layer net spin is aligned antiferromagnetically to those of the surface and subsurface layers.

Fig. 4. Calculated paramagnetic bands for fcc iron (001) 5 layer slab. The solid and dashed lines refer to + and - z (normal to the slab) reflection symmetries respectively. The darkened solid and dashed lines indicate states where the surface Fe weight is more than 50%. The even and odd symmetries in (a) and (b) refer to reflections about mirror planes through the corresponding high symmetry directions.

Fig. 5. Calculated spin-polarized bands for fcc iron (001) slab. (a) Even symmetry majority bands. (b) Even symmetry minority bands. (c) Odd symmetry majority bands. (d) Odd symmetry minority bands. The solid and dashed lines refer to + and - z (normal to the slab) reflection symmetries. The darkened solid and dashed lines show states where the surface Fe weight is more than 50%. The even and odd symmetries refer to reflections about the mirror planes through high symmetry directions.

Fig. 6. A comparison of the film derived bulk bands along Δ with those reported in Ref. 8. The open circles denote the states at $\bar{\Gamma}$ calculated for our paramagnetic, 5 layer fcc iron film.

The solid line is a guide to the eye. The dashed line connects calculated states (not shown here) that have been strongly affected by the surface compared to a bulk calculation. The vertical bars refer to experimental data from Ref. 8. The symmetry labels identifying the bands are also shown.

Fig. 7. A difference density contour plot of fcc Fe(001) and fcc Cu(001). This plot has been obtained by subtracting our (self-consistently) calculated fcc Cu(001) 5 layer film electron density from our calculated Fe/Cu(001) film electron density by aligning the surface layers. It should be used to compare differences in electronic density between the Cu(001) surface and the Fe/Cu(001) surface. The contours are labeled in units of 0.01 el/a_0^3. The numbers along the vertical and horizontal axes refer to distances in Bohr radii. The dotted regions show areas with increased electronic density. This change helps explain the work function increase calculated in going from 5 layers of Cu(001) to 5 layers of Fe(001) , both paramagnetic.

Fig. 8. A comparison of our calculated spin-polarized bands with ARUPS data of Ref.3. The open squares are the experimental data of Ref. 3. The upper panel (even symmetry) shows two pairs of calculated minority bands in + z reflection symmetry (dotted lines) and - z reflection symmetry (chain- dashed lines). The lower panel (odd symmetry) shows 4 pairs of our calculated bands, solid and dashed lines showing majority bands in + and - z reflection symmetries respectively while the dotted and chain-dashed lines show minority bands in + and - z reflection symmetries respectively. All the calculated bands shown here contain at least one state with 40% or more surface Fe weight.

Table I. Valence Charges , Magnetic Moments and Work Functions

Layer projected valence charges and magnetic moments together with the work functions of nonmagnetic and magnetic fcc iron 5 layers and nonmagnetic monolayer of iron on Cu(001). The values in parentheses are for the (2%) relaxed Fe/Cu(001) system.

	Fcc iron(para.)	Fcc iron(ferro.)	Fe/Cu(001)(para.)
Valence (el) : Center	7.20	7.20	(10.32) 10.32
Next to Center	7.16	7.17	(10.33) 10.33
Subsurface	7.16	7.17	(10.36) 10.34
Surface	6.98	6.96	(6.87) 6.95
Spin (μ_B) : Center	–	1.68 (↓)	–
Subsurface	–	2.30 (↑)	–
Surface	–	2.79 (↑)	–
Work Function (eV) :			
Present Theory	5.3	5.1	(5.5) 5.6
Experiment (Refs 6,7)	5.4	5.0	5.5

Table II. Contact Hyperfine Fields.

Fermi contact hyperfine fields in kG separated into core and valence contributions from various layers of the fcc iron slab. Note that the total contact field at the center layer nucleus is significantly lower than those at the surface and subsurface. The last row gives the ratio between the core contribution to the contact field and the respective magnetic moment.

	Center	Subsurface	Surface
Core	+209	-294	-359
Valence (4s)	-223	+39	+80
Total	-14	-255	-279
Core Field/Moment (kG/μ_B)	124	128	129

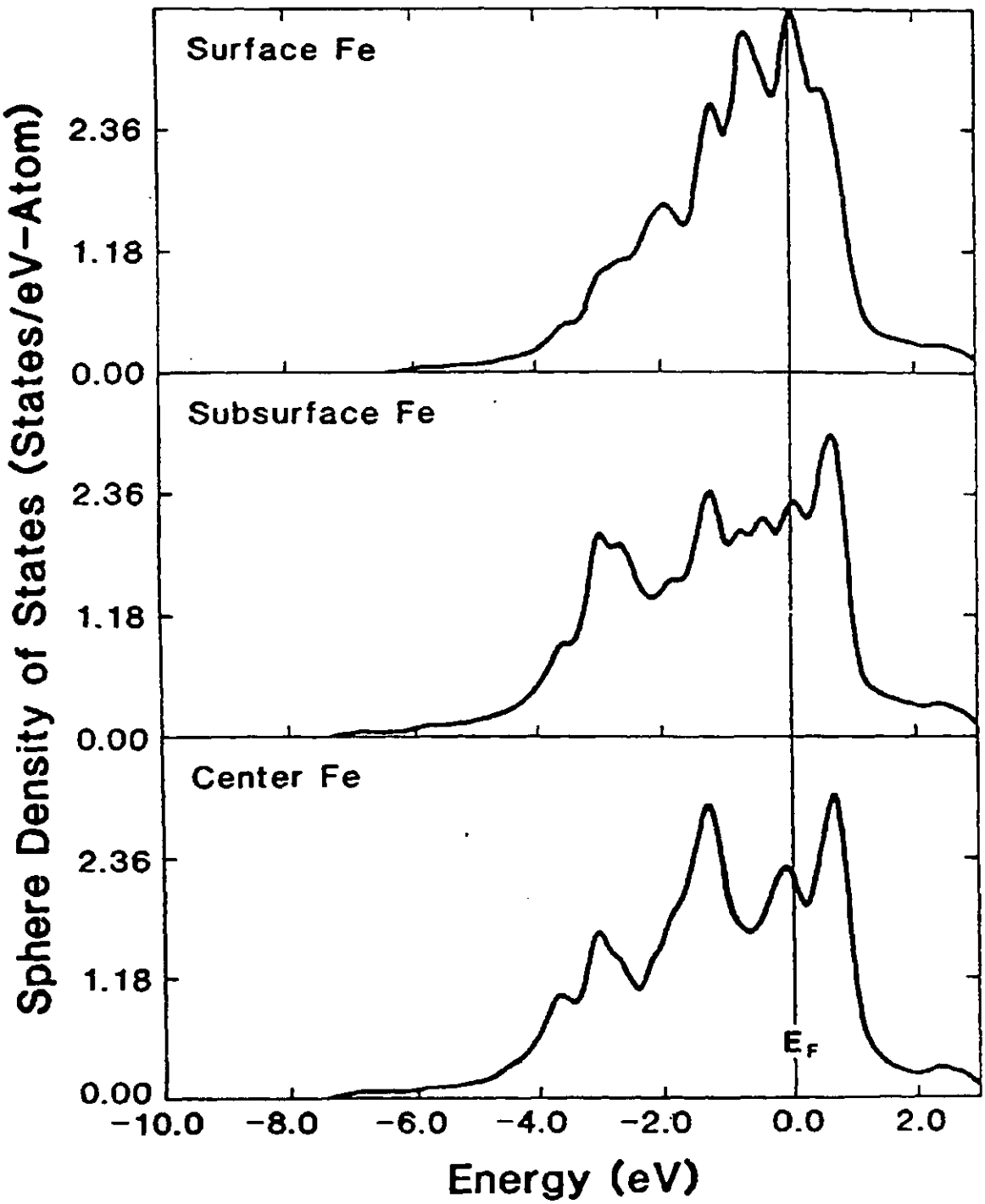
Surface Fe
Subsurface Fe
Center Fe
Sphere Density of States (States/eV-Atom)
2.36
1.18
0.00
E_F
−10.0
−8.0
−6.0
−4.0
−2.0
0.0
2.0
Energy (eV)

Fig. 1

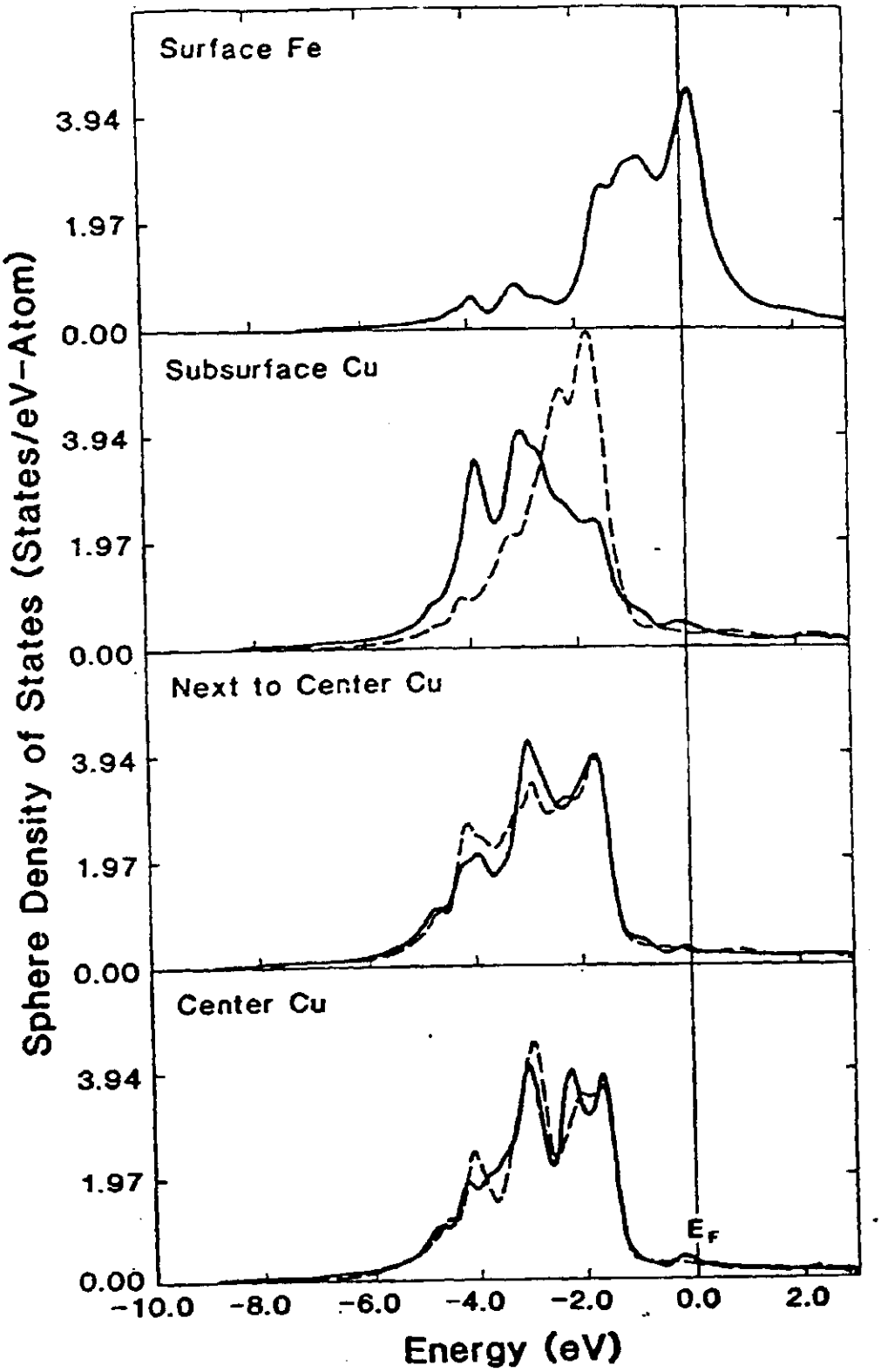
Surface Fe
Subsurface Cu
Next to Center Cu
Center Cu
3.94
1.97
0.00
Sphere Density of States (States/eV-Atom)
E_F
-10.0
-8.0
-6.0
-4.0
-2.0
0.0
2.0
Energy (eV)

Fig. #2

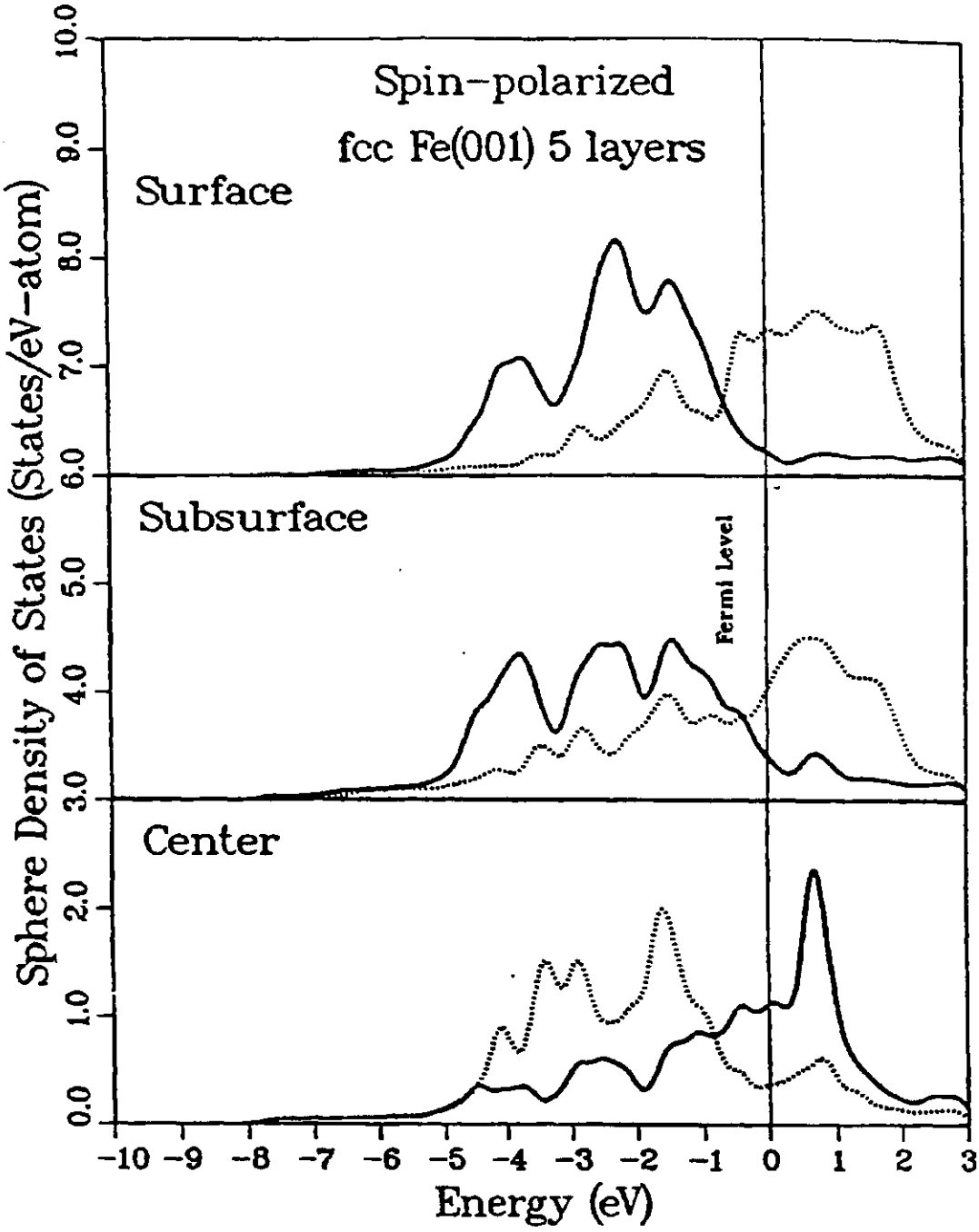
Spin-polarized
fcc Fe(001) 5 layers
Surface
Subsurface
Center
Fermi Level
Sphere Density of States (States/eV-atom)
Energy (eV)
0.0
1.0
2.0
3.0
4.0
5.0
6.0
7.0
8.0
9.0
10.0
-10 -9 -8 -7 -6 -5 -4 -3 -2 -1 0 1 2 3

Fig. #3

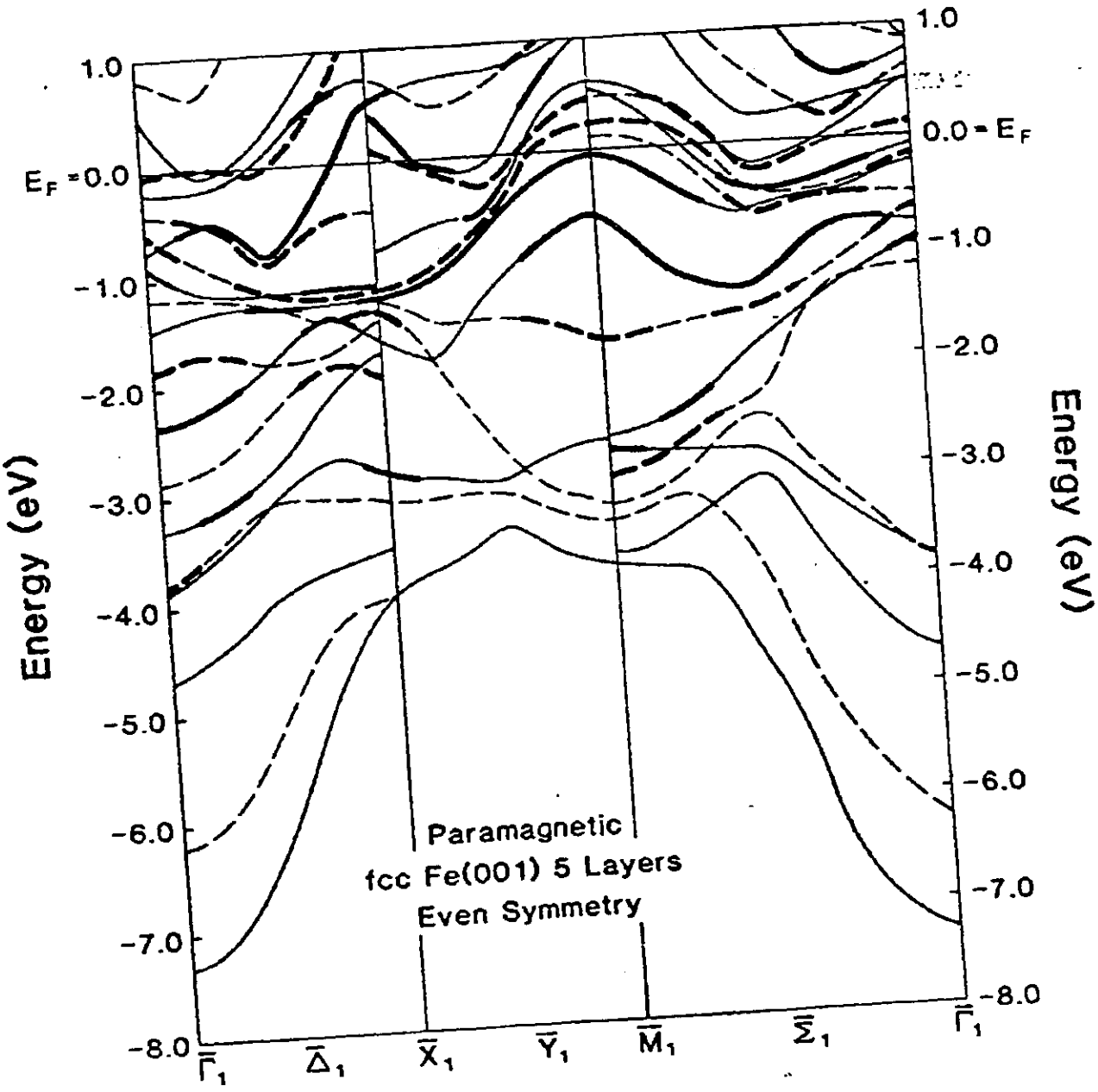
1.0
E_F = 0.0
-1.0
-2.0
-3.0
-4.0
-5.0
-6.0
-7.0
-8.0
Energy (eV)
1.0
0.0 = E_F
-1.0
-2.0
-3.0
-4.0
-5.0
-6.0
-7.0
-8.0
Energy (eV)
Paramagnetic
fcc Fe(001) 5 Layers
Even Symmetry
$\bar{\Gamma}_1$
$\bar{\Delta}_1$
$\bar{X}_1$
$\bar{Y}_1$
$\bar{M}_1$
$\bar{\Sigma}_1$
$\bar{\Gamma}_1$

Fig. 4a

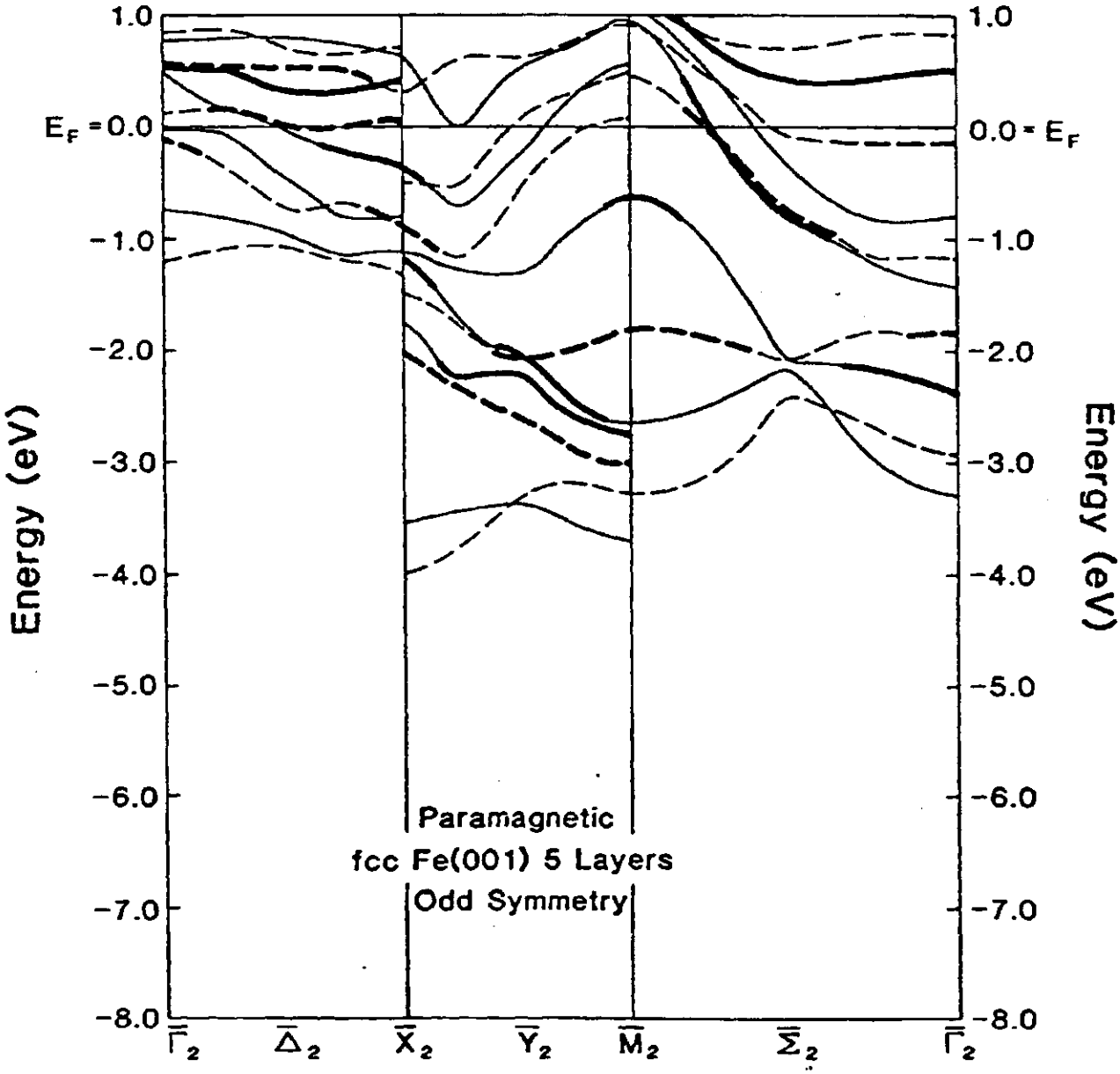
1.0
E_F = 0.0
-1.0
-2.0
-3.0
-4.0
-5.0
-6.0
-7.0
-8.0
Energy (eV)
1.0
0.0 = E_F
-1.0
-2.0
-3.0
-4.0
-5.0
-6.0
-7.0
-8.0
Energy (eV)
Paramagnetic
fcc Fe(001) 5 Layers
Odd Symmetry
$\bar{\Gamma}_2$
$\bar{\Delta}_2$
$\bar{X}_2$
$\bar{Y}_2$
$\bar{M}_2$
$\bar{\Sigma}_2$
$\bar{\Gamma}_2$

Fig. 4b

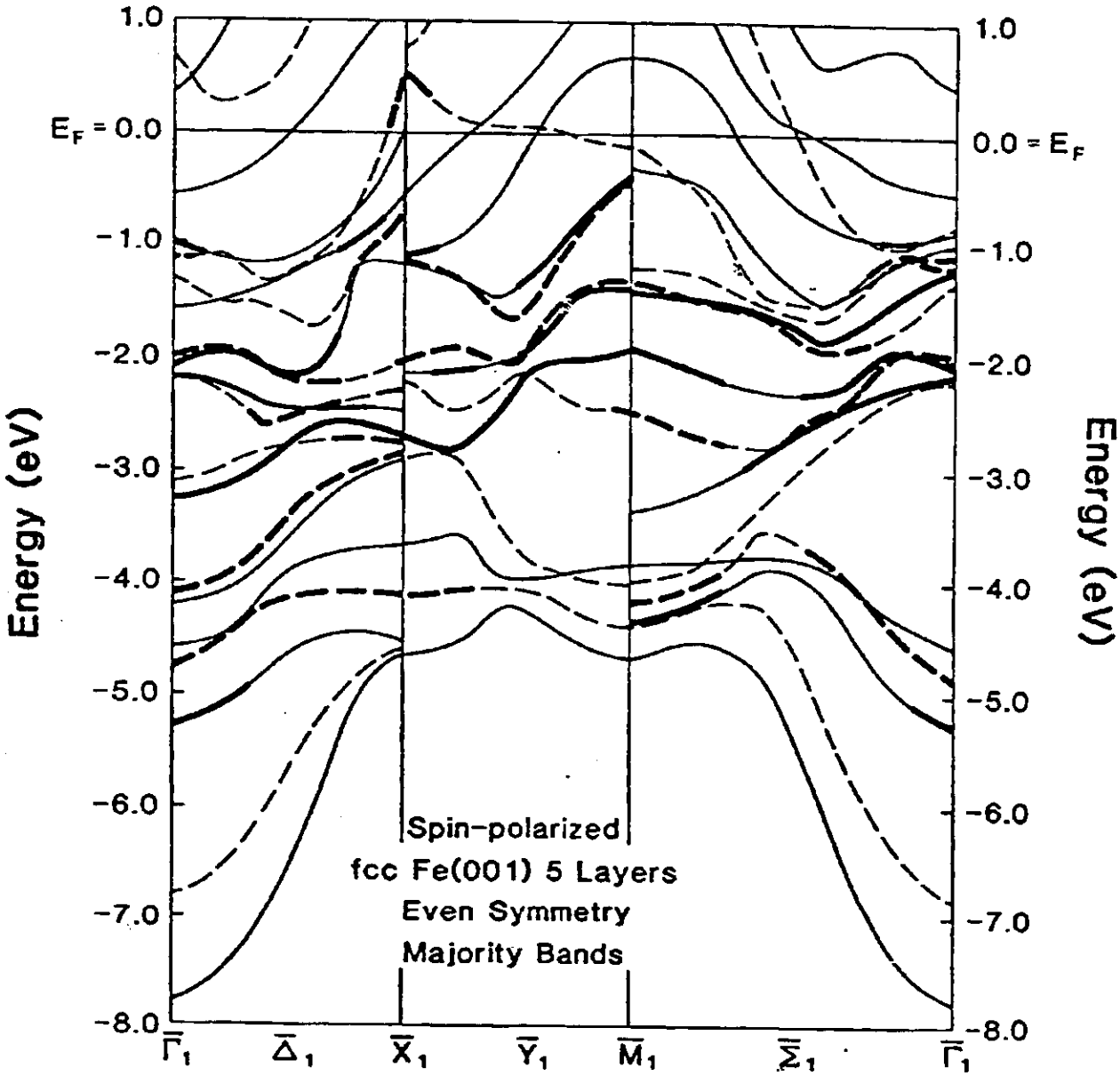
1.0
E_F = 0.0
-1.0
-2.0
-3.0
-4.0
-5.0
-6.0
-7.0
-8.0
Energy (eV)
1.0
0.0 = E_F
-1.0
-2.0
-3.0
-4.0
-5.0
-6.0
-7.0
-8.0
Energy (eV)
Spin-polarized
fcc Fe(001) 5 Layers
Even Symmetry
Majority Bands
$\bar{\Gamma}_1$
$\bar{\Delta}_1$
$\bar{X}_1$
$\bar{Y}_1$
$\bar{M}_1$
$\bar{\Sigma}_1$
$\bar{\Gamma}_1$

Fig. 5a

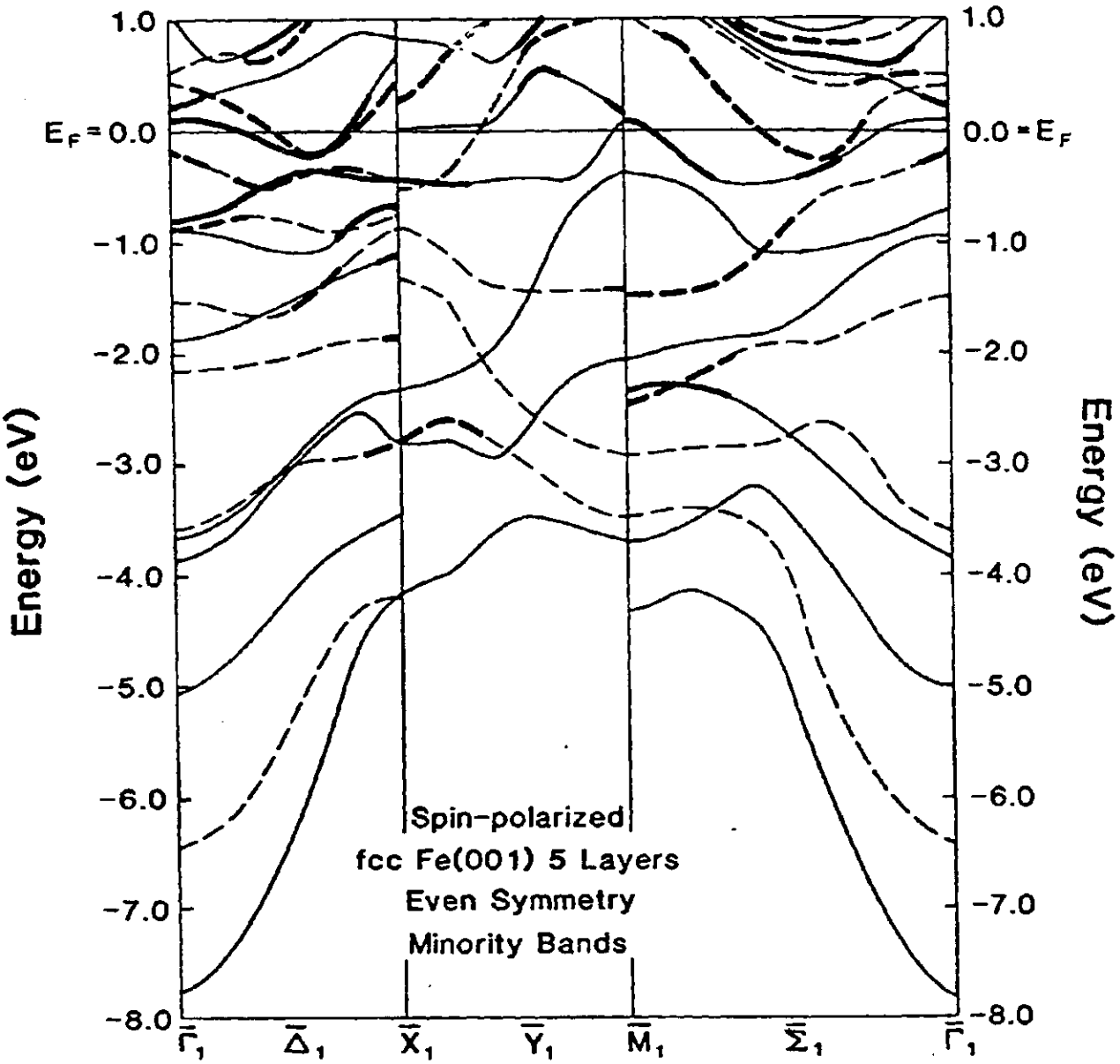
1.0
$E_F = 0.0$
-1.0
-2.0
-3.0
-4.0
-5.0
-6.0
-7.0
-8.0
Energy (eV)
1.0
$0.0 = E_F$
-1.0
-2.0
-3.0
-4.0
-5.0
-6.0
-7.0
-8.0
Energy (eV)
Spin-polarized
fcc Fe(001) 5 Layers
Even Symmetry
Minority Bands
$\bar{\Gamma}_1$
$\bar{\Delta}_1$
$\bar{X}_1$
$\bar{Y}_1$
$\bar{M}_1$
$\bar{\Sigma}_1$
$\bar{\Gamma}_1$

Fig. 5b

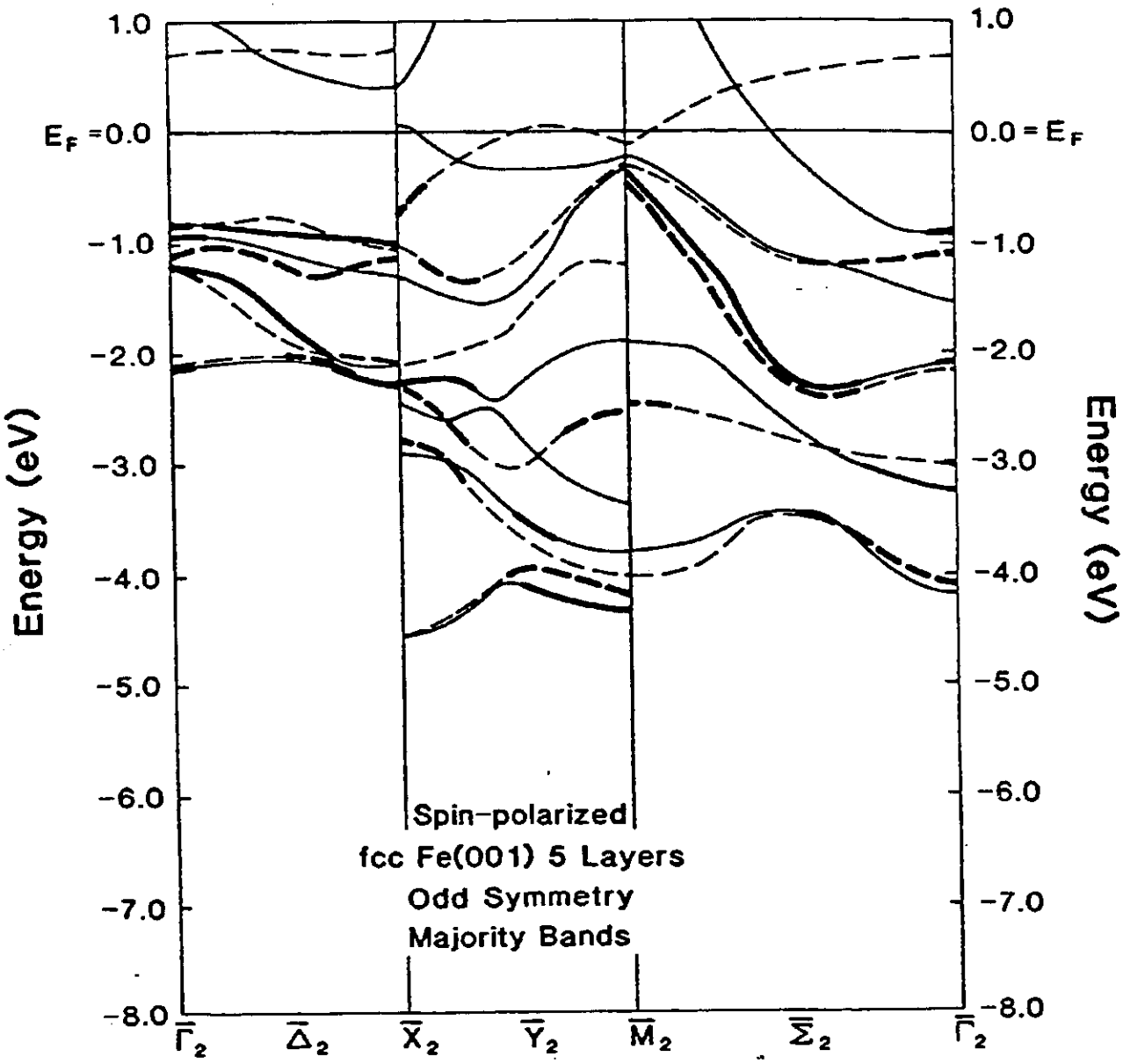
1.0
E_F =0.0
-1.0
-2.0
-3.0
-4.0
-5.0
-6.0
-7.0
-8.0
Energy (eV)
1.0
0.0 = E_F
-1.0
-2.0
-3.0
-4.0
-5.0
-6.0
-7.0
-8.0
Energy (eV)
Spin-polarized
fcc Fe(001) 5 Layers
Odd Symmetry
Majority Bands
$\bar{\Gamma}_2$
$\bar{\Delta}_2$
$\bar{X}_2$
$\bar{Y}_2$
$\bar{M}_2$
$\bar{\Sigma}_2$
$\bar{\Gamma}_2$

Fig. 5C

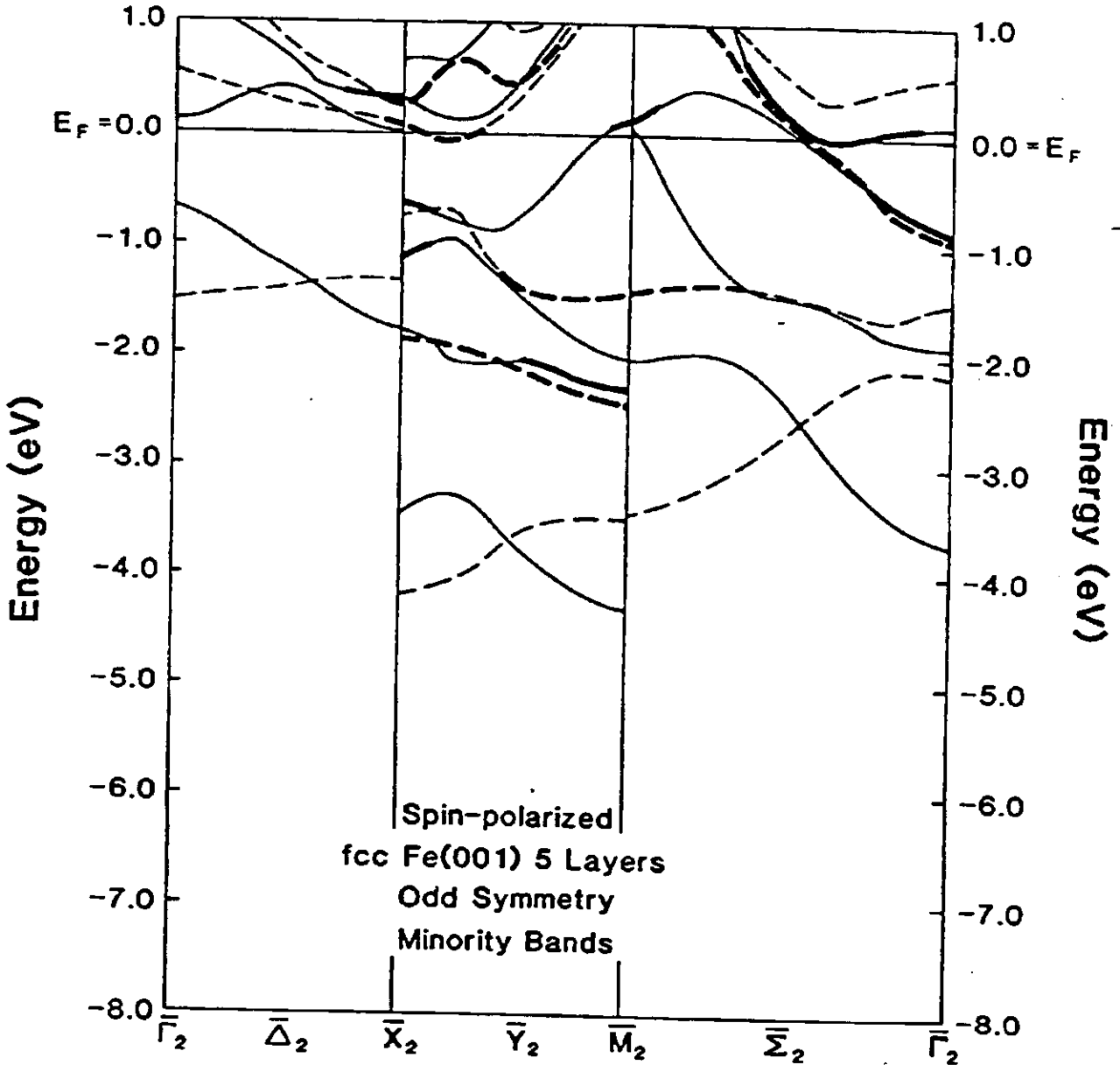
1.0
E_F = 0.0
-1.0
-2.0
-3.0
-4.0
-5.0
-6.0
-7.0
-8.0
Energy (eV)
1.0
0.0 = E_F
-1.0
-2.0
-3.0
-4.0
-5.0
-6.0
-7.0
-8.0
Energy (eV)
Spin-polarized
fcc Fe(001) 5 Layers
Odd Symmetry
Minority Bands
$\bar{\Gamma}_2$
$\bar{\Delta}_2$
$\bar{X}_2$
$\bar{Y}_2$
$\bar{M}_2$
$\bar{\Sigma}_2$
$\bar{\Gamma}_2$

Fig. 5d

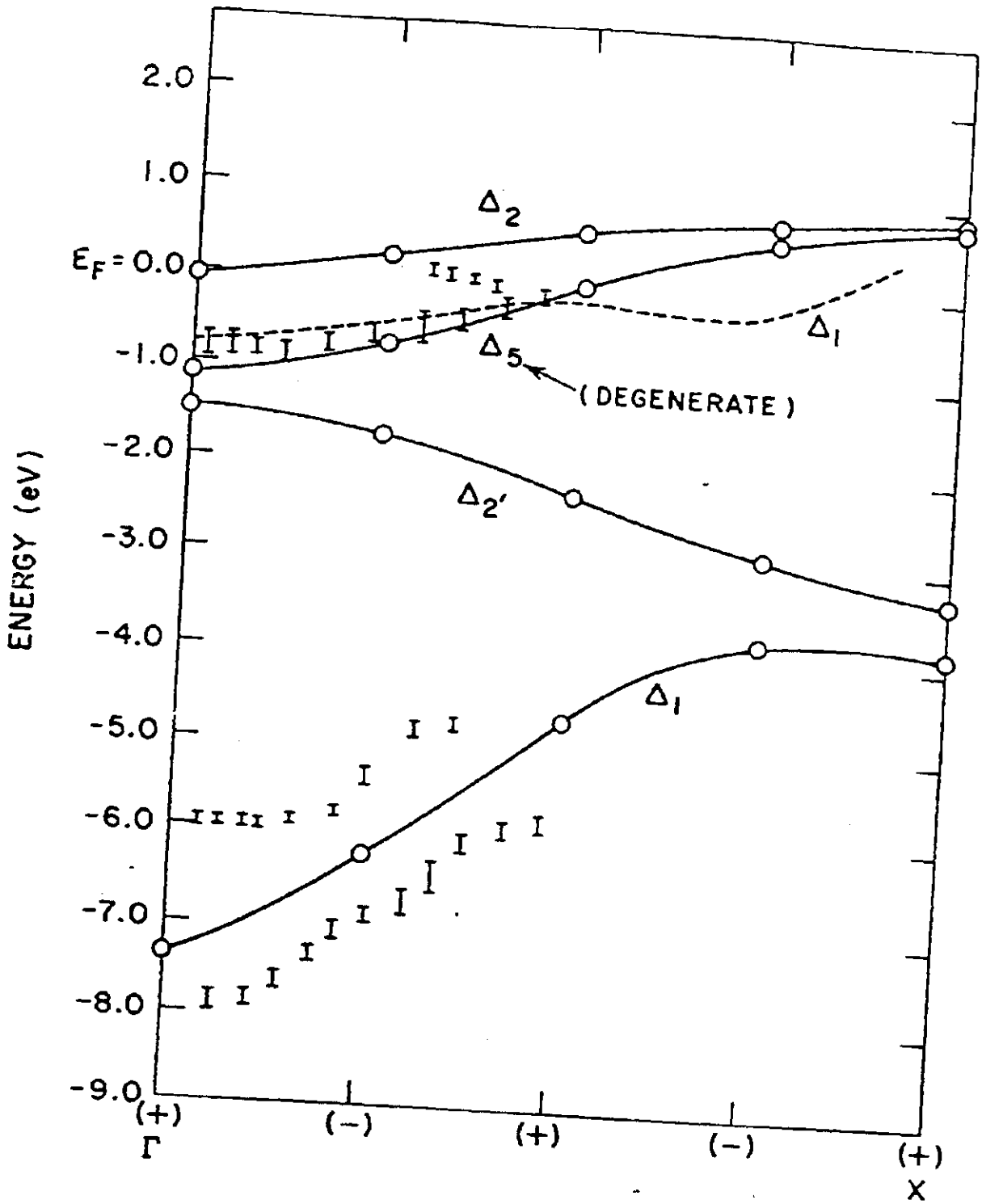
2.0
1.0
$E_F = 0.0$
-1.0
-2.0
-3.0
-4.0
-5.0
-6.0
-7.0
-8.0
-9.0
ENERGY (eV)
Δ_2
Δ_1
Δ_5
(DEGENERATE)
$\Delta_{2'}$
Δ_1
(+)
Γ
(−)
(+)
(−)
(+)
X

Fig. #6

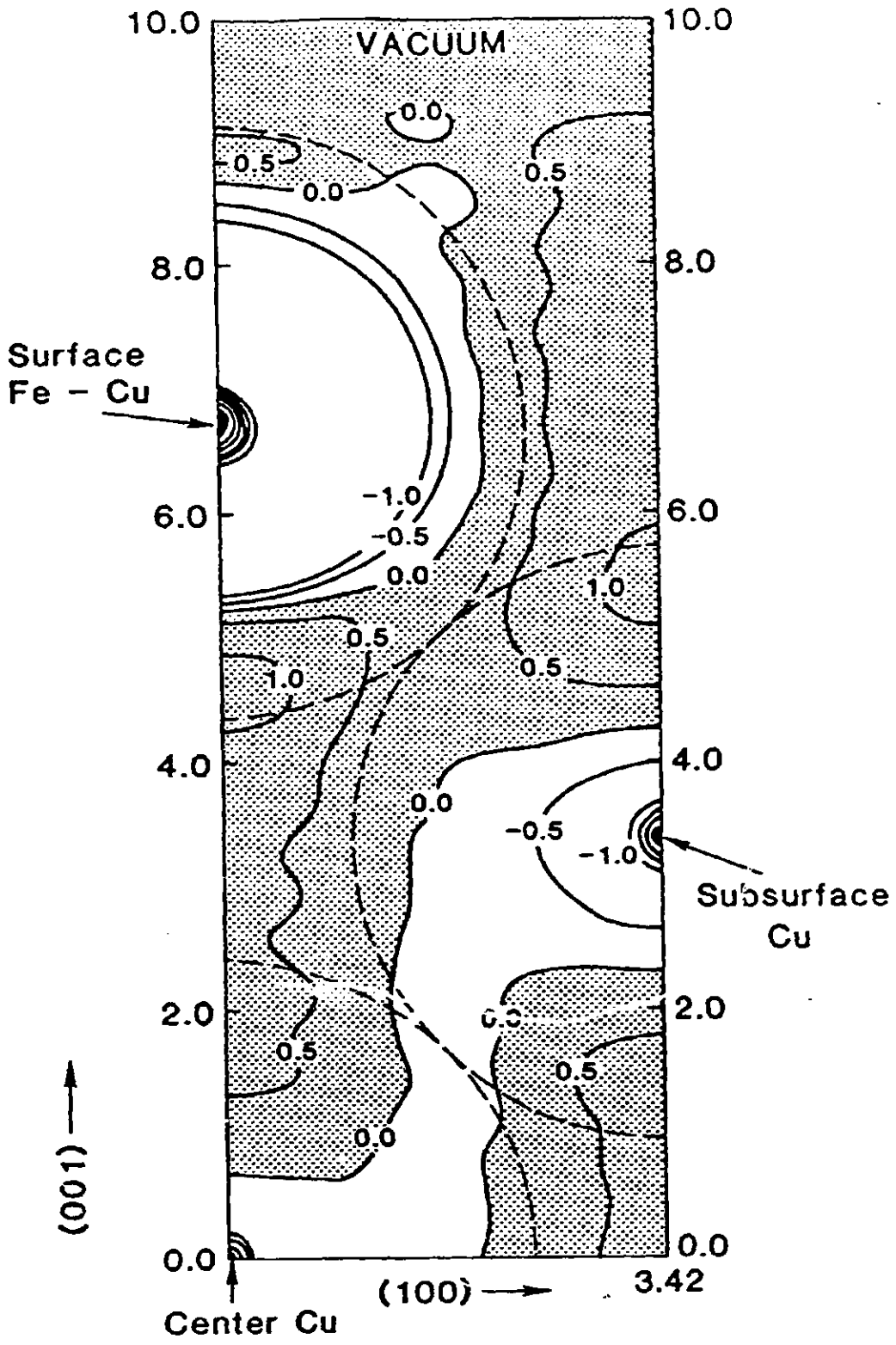
10.0
VACUUM
10.0
0.0
-0.5
0.0
0.5
8.0
8.0
Surface
Fe – Cu
-1.0
-0.5
0.0
6.0
6.0
1.0
0.5
0.5
1.0
4.0
4.0
0.0
-0.5
-1.0
Subsurface
Cu
2.0
2.0
0.5
0.0
0.5
0.0
(001)
0.0
0.0
3.42
(100)
Center Cu

Fig. 7

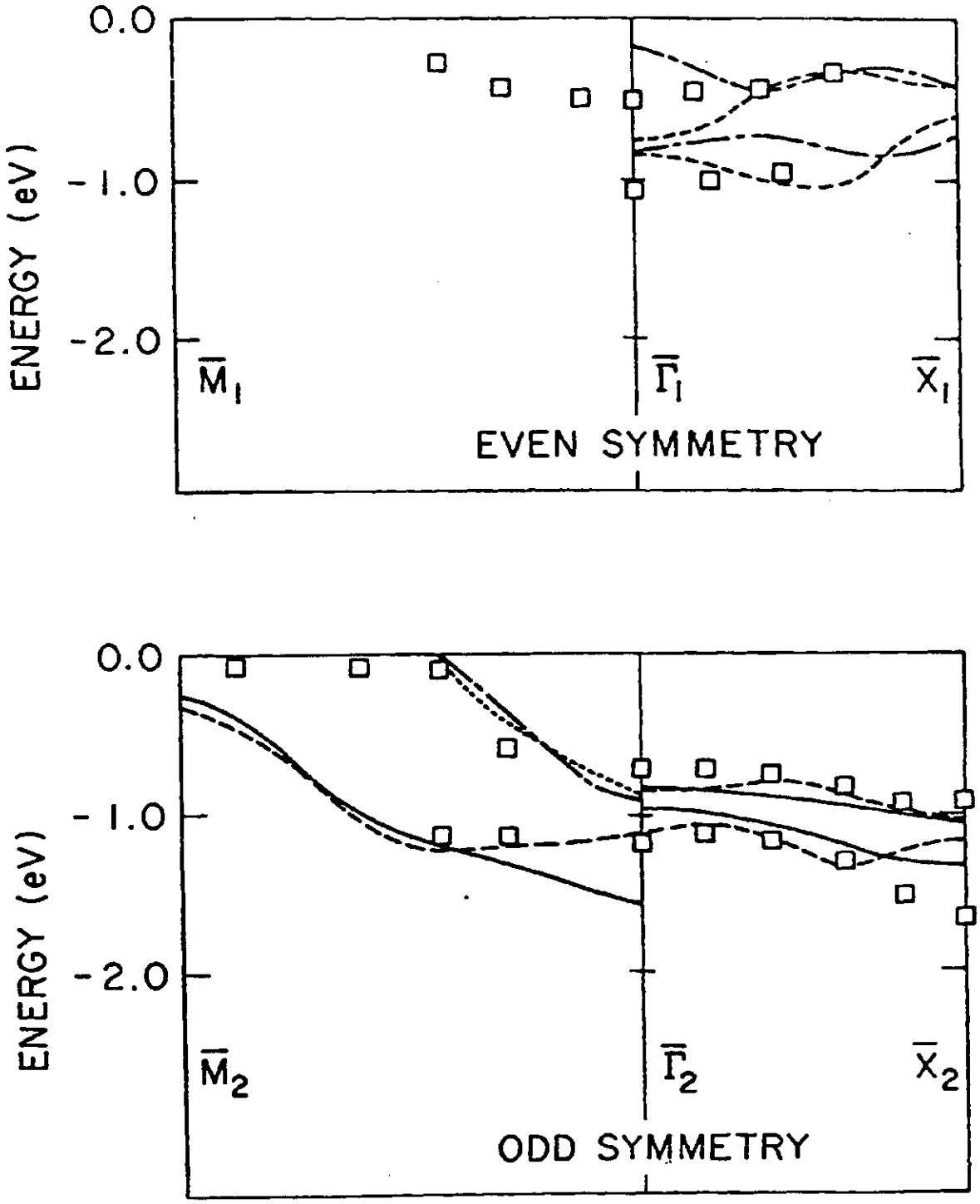
0.0
-1.0
-2.0
ENERGY (eV)
$\bar{M}_1$
$\bar{\Gamma}_1$
$\bar{X}_1$
EVEN SYMMETRY
0.0
-1.0
-2.0
ENERGY (eV)
$\bar{M}_2$
$\bar{\Gamma}_2$
$\bar{X}_2$
ODD SYMMETRY

Fig # 8

3. LEED MEASUREMENTS OF Fe EPITAXIALLY GROWN ON Cu(100)

(Quarterly Report April 16, 1986 - July 15, 1986)

ABSTRACT

Iron was epitaxially grown on a Cu(100) surface. Low energy electron diffraction (LEED) intensity versus energy curves were recorded for one and ten layers of iron on Cu(100) at room temperature. A full dynamical analysis was performed using the renormalized forward scattering perturbation method. The Debye temperatures for 1 and 10 layers were determined from the temperature dependence of the (00) beam. The surface Debye temperatures determined by this method were 233K for 1 ML Fe and 380 K for 10 L of Fe. The value obtained for fcc iron was 550 K. A multiple relaxation approach was employed in analyzing the experimental data. The estimated interlayer spacings for the first and second layers were 1.78 $\pm$ 0.02 Å(first) and 1.81 $\pm$ 0.02 Å(second) for 1 ML Fe, and 1.81 $\pm$ 0.02 Å (first) and 1.78 $\pm$ 0.02 Å (second) for 10 layers of Fe on Cu(100). Auger electron spectroscopy was used to determine the thickness of the Fe films, and the LEED measurements indicate approximately a layer-by-layer growth until about 17 layers at room temperature. At higher temperatures there is evidence of iron diffusion or copper surface seggregation.